INTERNATIONAL JOURNAL OF
ADVANCED SCIENTIFIC RESEARCH AND INNOVATION

ISSN: 2785-9541 VOLUME 2, ISSUE 1, 2021, 1 – 20. www.egyptfuture.org/ojs/

Dependence of Particle Size and Shape of Polyaniline Nanoparticle on the Time of Ultrasonic Irradiation Reaction

R.Seoudi[a,b] , A.EL-Bialy[c] , A. A. Shabaka[a] and N.M.Farrage[a]

a Spectroscopy Department, Physics research Institute, National Research Centre, Dokki , Cairo 12622, Egypt

b Physics Deptartment, Faculty of Science, Umm Al-Qura University, Makkah, Saudi Arabia

c Physics Deptartment, Faculty of Girls, Ain-Shams University, Cairo, Egypt

Abstract

In this article, polyaniline (PANI) nanoparticles in the uniform size (3.2-10 nm in diameter) were successfully prepared by ultrasonic irradiation method at different times in the presence of hydrochloric acid as a dopant and ammonium peroxydisulfate (APS) as an oxidant. The dependence of particle size, morphologies, and crystallinity on the time of ultrasonic irradiation reaction was studied using transmission electron microscope (TEM) images, and X-ray diffraction (XRD). The data indicated that, the particle size was increased with increasing the time of reaction. The vibrational structure and electronic transition were studied using FTIR and UV-VIS spectroscopic techniques. All data confirmed that, the particle size of polyaniline nanoparticle was increased with increasing the time of ultrasonic irradiation reaction.

Keywords: PANI nanoparticles; ultrasonic irradiation; X-ray diffraction; TEM; FTIR, UV/VIS spectroscopic techniques.

ISSN: 2785-9541 VOLUME 2, ISSUE 1, 2021, 1 – 20. www.egyptfuture.org/ojs/

1. Introduction

Polyaniline has been most extensively studied because it exhibits easy of preparation, good environmental stability and its electrical, thermoelectric, and optical properties can be modified by the oxidation state of the main chain and degree of protonation **(1-3)**. Polyaniline (PANI) is viewed as organic metals due to their metallic-like conductivity combined with the processability of organic polymers **(4)**. Polyaniline has possible applications in rechargeable batteries, corrosion protection, light emitting diodes, molecular sensors, electrochromic devices and microwave screening **(5)**. The unique non-redox acid/base (doping/dedoping) chemistry of PANI and its consequence on structural, spectroscopic, and electronic transport properties allows PANI to be versatile in its end properties **(4)**. The design of the dopant not only increases electronic conductivity, but also alters electronic transport, processability, and optical properties. This dopant was shown to have consequences on polyaniline's morphology at the nano-scale**(4)**. The spectral characteristics are the evidence for their peculiar behavior at nano dimensional level. Thermo physical and mechanical properties of polymers have inherently shown dimension dependence **(6)**. One-dimensional nanostructures of conducting polymers have attracted intensive interest because of their novel physical properties and potential applications such as chemical sensors **(7-9),** polymeric conducting molecular wires, **(10)** gas-separation membranes **(11,12)** and neuron devices**(13)**. Polyaniline (PANI) is one of the most important conducting polymers and

ISSN: 2785-9541 VOLUME 2, ISSUE 1, 2021, 1 – 20. www.egyptfuture.org/ojs/

the most promising systems for nanoelectronic applications **(14)**. In recent years, one-dimensional (1-D) PANI nanostructures have attracted much research interest since they are a kind of desirable molecular wire due to their 1-D structure, metal-like and controllable conductivity. Different morphologies of PANI have been obtained through different synthesis or processing routes. In general, 1-D PANI nanostructures are synthesized chemically or electrochemically through a "template synthesis" route **(15)**. Ngamna and Morrin **(16)** prepared aqueous polyaniline (PANI) nanoparticles doped with dodecylbenzenesulfonic acid (DBSA) as surfactant with size ~80 nm. Kim [(17)] prepared PANI nanoparticles of size 10-20 nm by oxidation with ammonium peroxydisulfate(APS) in sodium dodecylsulfate(SDS) micellar solutions, where the role of SDS as a surfactant which controlled the size of PANI particles . Fundamental understanding of, how size and morphological changes influence the physico-chemical properties of polyaniline nanoparticles are of great technological interest. To achieve this, it is required to obtain polyaniline nanoparticles in varied dimensions and morphologies. It has been observed frequently that the ultimate size, morphology and shape of polyaniline nanoparticles are highly subjective to the reaction conditions. This work was focused on the preparation and controlling the nanoparticle sizes of PANI-HCl without any surfactants by changing the time of ultrasonic irradiation reaction. The effect of ultrasonic irradiation reaction time on the particle size, morphology, vibrational and optical properties was investigated.

2. Experimental

2.1Preparation of PANI nanoparticles with different sizes

ISSN: 2785-9541 VOLUME 2, ISSUE 1, 2021, 1 – 20. www.egyptfuture.org/ojs/

Polyaniline nanoparticles were synthesized by ultrasonic irradiation method. A typical synthesis process for PANI/Hcl nanoparticles is as follows. 2.14 ml of aniline monomer (Fluka 99.5%) and 6 ml of Hcl (37%) as a dopant were added together to 111 ml deionized water at 15 ^{o}C. Then 2.768g ammonium peroxysulfate (APS) as an oxidant dissolved in 16 ml deionized water was added through dropwise method approximately 10 min. After the addition of the oxidant, the colorless homogeneous solution slowly turns to blue, green and then to dark green. The reaction mixture was kept 30 min under ultrasonic irradiation. The mixture was left overnight in ice box. At the end, the dark green precipitate were obtained and separated by centrifuging at 4000 rpm, washed with deionized water, methanol and ether three times respectively, to remove the nonreacted chemicals and then the samples were dried at 35 ◦C for 12 h. The ultrasonic irradiation reaction time was varied from 30 to 120 min to prepare doped polyaniline in nano-size dimension with different sizes and shapes.

2.2 Samples characterization

A Transmission Electron Microscope (JEOL-JEM 2010) operated at 200 kV accelerating voltage was used to study the morphology, shape and particle size distribution. The samples were prepared by making a suspension from the powder in distilled water using ultrasonic water bath. Then a drop of the suspension was put into the carbon grid and left at room temperature to evaporate the solvent. X-ray data was recorded using (X-Ray Differaction-D8 advance X-ray differactometer; Bruker AXS) operated at (40K V and 40mA) using CuKα radiation of wavelength (λ=1.5406A) at 25OC and

ISSN: 2785-9541 VOLUME 2, ISSUE 1, 2021, 1 – 20. www.egyptfuture.org/ojs/

2θ=20-80O with a step size of 0.04 O and a scanning speed of 1o /min. The vibrational spectra were measured in the wavenumber range (4000-350 cm-1) using Jasco 6100 Fourier transform infrared (FTIR) Spectrometer. The samples were measured in mid-IR range using KBr method. Optical absorption spectra of doped PANI nanoparticles suspension in water were recorded in the absorbance mode using Jasco spectrometer (UV-VIS-NIR 570, Japan) at a resolution of 2 nm.

3. Results and Discussion

3.1 Transmission electron microscopy (TEM) data

Transmission electron microscope (TEM) images of PANI prepared at different ultrasonic irradiation reaction time (oxidation time) from 30 to 120 minutes were shown in Figure (1: a-d). From these images, it is clear that, spherical shapes with regular distribution of PANI were synthesized in nanoform with different sizes (3.2 - 10 nm). The size of the particles was affected by oxidation time such that, the size of particles was increased with increasing the oxidation time and the spherical morphologies were still preserved. First, when the initial oxidation time was 30 min, the size of nanoparticles obtained is in the range of 3.2 – 4.9 nm and after the oxidation time was increased to 120 min, the size was increased (7 -10 nm). When the oxidation time was small, the reaction was mild and the aggregation of nuclei did not take place lead to the formation of particles smaller in size. At long time of oxidation, the reasons may be due to the formation mechanism of the primary nuclei (anilinium cation in acidic aquose solution) in the acidic media was rapid at higher oxidation time. These lead to the agglomerations of nuclei and subsequently increase the size of the particles.

INTERNATIONAL JOURNAL OF
ADVANCED SCIENTIFIC RESEARCH AND INNOVATION

ISSN: 2785-9541 VOLUME 2, ISSUE 1, 2021, 1 – 20. www.egyptfuture.org/ojs/

INTERNATIONAL JOURNAL OF
ADVANCED SCIENTIFIC RESEARCH AND INNOVATION

ISSN: 2785-9541 VOLUME 2, ISSUE 1, 2021, 1 – 20. www.egyptfuture.org/ojs/

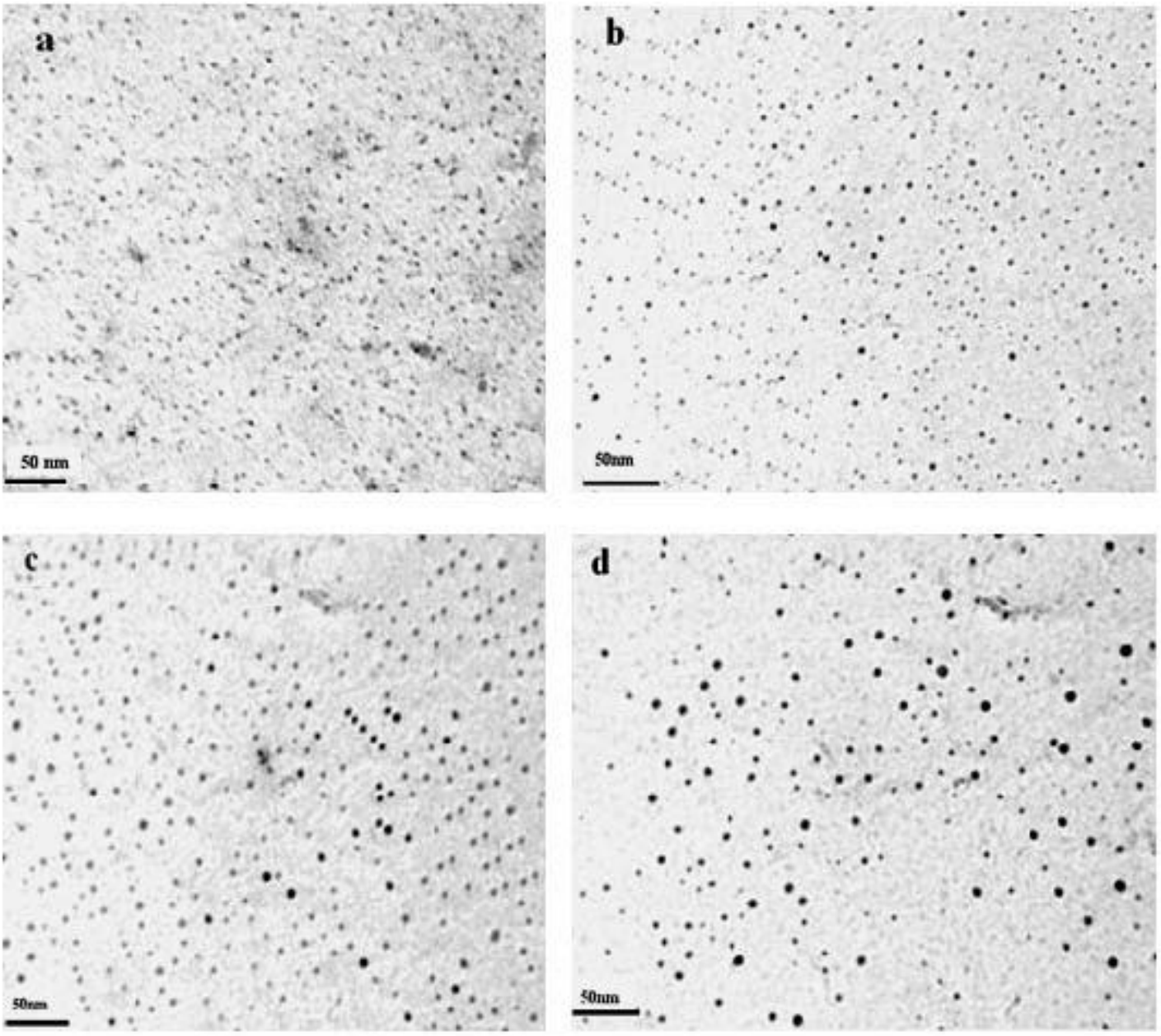

Figure (1): Transmission electron microscope images of PANI nanoparticles prepared at different oxidation times (a) 30 min, (b) 60 min, (c) 90 min, (d) 120 min.

ISSN: 2785-9541 VOLUME 2, ISSUE 1, 2021, 1 – 20. www.egyptfuture.org/ojs/

3.2. X-Ray diffraction

Figure 2 shows the X-Ray diffraction (XRD) pattern of the PANI/Hcl nanoparticles prepared at different oxidation times (30, 60, 90 and 120 min). From this pattern it can be observed that, at oxidation state was 30 min, three broad diffraction peaks centered at 2θ around 15.21°, 20.05° and 25.17°. The first one was characterized of the diffraction of an amorphous polyaniline polymer. The broad amorphous peak centered at 20.05° may be ascribed to periodicity parallel to the polymer chain. Abdiryim et al **(18)** discussed this peak as a distance between the ring planes of benzene rings in adjacent chains or the close-contact interchain distance. The crystalline peak at 2θ ~25.17◦ was represented the polyaniline nanoparticle and it may be caused by the periodicity perpendicular to the chain polymer direction. This is agreed with the previous work **(19-22)**. By comparing the two peaks at 2θ =~25.17◦ and 2θ =~20.05◦ it was found that, the first peak was stronger than that of the last peak. This indicated that the PANI was in the form of highly doped emeraldine salt and had good crystallinity.

ISSN: 2785-9541 VOLUME 2, ISSUE 1, 2021, 1 – 20. www.egyptfuture.org/ojs/

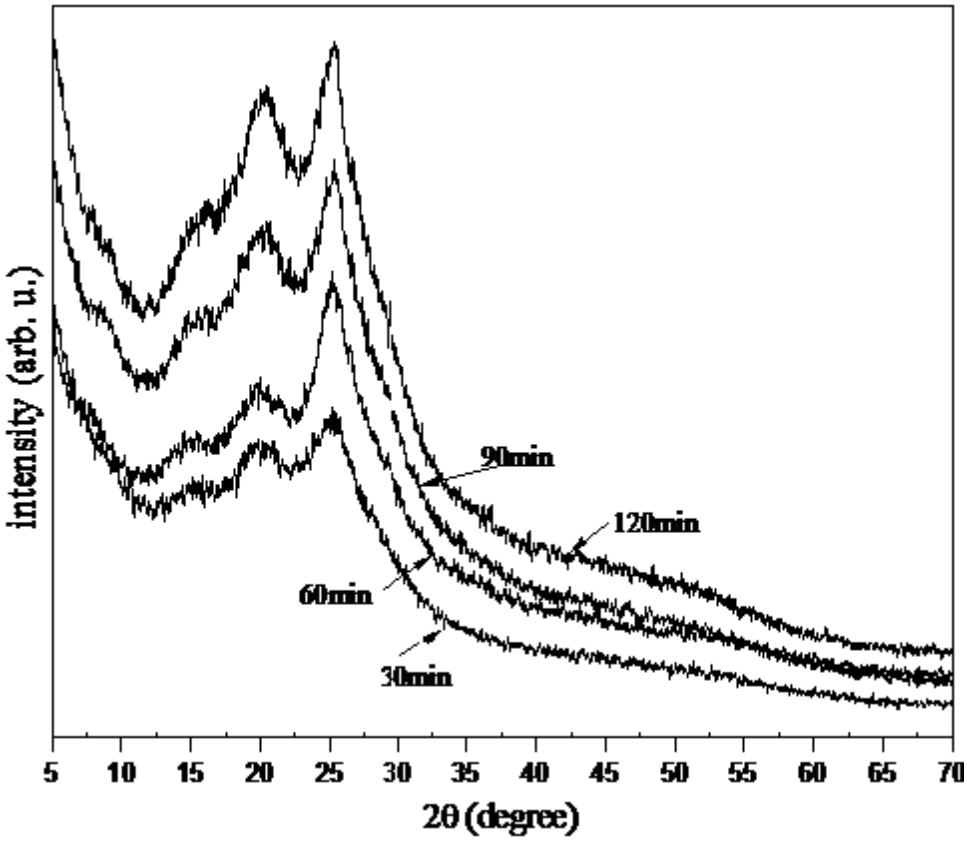

Figure 2: X-ray diffraction of polyaniline nanoparticle prepared at different oxidation times (30, 60, 90, and 120 min).

3.2.1. Effect of oxidation time on the crystallinity and particle size of PANI

Crystallinity and orientation of PANI have been of much interest, because more highly ordered systems can display a metallic behaviour. In our work X-ray diffractogram was used to study the degree of crystallinity, particle size, inter-chain separation and the d-spacing. The percentage crystallinity was estimated as the area of diffractogram under the crystalline peaks

ISSN: 2785-9541 VOLUME 2, ISSUE 1, 2021, 1 – 20. www.egyptfuture.org/ojs/

divided by the total area of the diffractogram using the following relation**(23)**.

$$\left(\text{Crystallinity } \% = \frac{S_{cryst.}}{S_{total}} \text{x} 100\%\right)$$

The d-spacing of different samples was determined by Debyee Scherrer (powder) method using Bragg's relation ($n\lambda=2d\sin\theta$) **(24)**, where λ is X-ray wavelength, n is an integer number. We use n=1 in the above equation because for $n \geq 2$ the X-ray diffraction signal intensity will be much lower than for n = 1, and θ is the angle of deviation of the diffracted beam, and is measured in the plane of the incident and diffracted beams. The particle size D was determined from the XRD pattern according to the Scherrer's equation

$$\left(\mathrm{D} = \frac{K\lambda}{\beta \cos\theta}\right)$$

where D is the particle size, K is the shape factor for the particle (~0.9), β is the full width at half maxima of the crystalline peak in radians. The inter-chain separation was determined from the relation given by Klug and Alexander **(25)**

$$\left(\mathrm{R} = \frac{5\lambda}{8 \sin\theta}\right)$$

where, R is the inter-chain separation. The degree of crystallinity, particle size, inter-chain separation and the d-spacing of PANI nanoparticles prepared at different oxidation times (30, 60, 90, 120 min) were calculated

ISSN: 2785-9541 VOLUME 2, ISSUE 1, 2021, 1 – 20. www.egyptfuture.org/ojs/

from all patterns (Figure 2) using the above equations and listed in Table (1). From this table, it is clear that; with the increasing of the oxidation time the degree of crystallinity and particle size are increased, where the d-spacing and inter-chain separation are decreased. The ratio of the intensities at 20.05° and $I_{25.17}/ I_{20.05}$, increased with the increase in crystallinity. All these may be due to the conformational changes of the polymer chain and it was obtained from the increased of the amorphous scattering at 2θ of 20°.05. Further manifested by a remarkable increase in crystalline peaks centered 25.05° compared to the pattern of the sample at oxidation time 30 min. The crystalinity increased with the particle size increased, the reason is that the PANI nanoparticles prepared in small sizes with different times and still small where the largest particle size at oxidation time 120 min is 10 nm. The crystallinity and the structure of PANI nanoparticles are affected by the oxidation state of the polymer [(26)]. Due to the polymerization of aniline in aqueous solution during increased oxidation time could proceed in denser and more compact structure. The aggregation and stacking of the PANI chains depend on the hydrogen bonding between the imine and amine nitrogen sites. This means that; the system contains highly ordered polymer chains. This depends on the inter-chain hydrogen bonding or electrostatic (dipole–dipole) interaction existing among adjacent polymer chains [(27)].

ISSN: 2785-9541 VOLUME 2, ISSUE 1, 2021, 1 – 20. www.egyptfuture.org/ojs/

Table (1): Estimated values of d-spacing, inter-chain separation, particle size of PANI nanoparticles and the degree of crystallinity at different oxidation times.

Time	2θ(°)	d(A°)	R(A°)	Particle size(nm)	Crystallinity	Ratio (I25.17/I20.05)
30 min	25.17	3.5353	4.4191	2.3	53.1	1.12256
60 min	25.21	3.5298	4.4122	4.4	54.97	1.28996
90 min	25.26	3.5229	4.4036	5.7	57.46	1.3652
120 min	25.32	3.5147	4.3934	7.1	59.75	1.47874

3.3. FTIR spectroscopic data

The FTIR spectra of the PANI nanoparticles prepared at oxidation times (30, 60, 90 and 120 min) in the wavenumber range from 4000- 400 cm-1 was illustrated in Figure (3). The broad absorption band around 3440 cm-1 is characteristic of the stretching vibration of hydrogen bond (O-H) of the absorbed water by the prepared samples. The weak band appeared at about 3233 cm-1 was refereed to N-H stretching vibration in secondary amine **(28)**. This band was indicated the presence of charged amine or imine species. The two bands appeared at 1575 cm-1 and 1492 cm-1 were corresponded to N=Q=N and N-B-N stretching vibrations of quinone and benzene ring respectively. The appearances of these two bands were indicated to the formation of polyaniline (PANI)**(29,30)**. Their positions were independent of doped or undoped form of polyaniline but the intensity ratio was reflected to the content of the quinoid imine and benzene ring structure. The band at 1300 cm-1 was assigned to C-N stretching vibration in the quinoid imine unit. The band at 1249 cm-1 ascribed to the C-N+.

ISSN: 2785-9541 VOLUME 2, ISSUE 1, 2021, 1 – 20. www.egyptfuture.org/ojs/

stretching vibration in the polaron structure and it was indicated that the PANI was in a doped state and it was agreed with the previous work **(28,31-33)**. Also, this characteristic band confirms that the PANI salts contain the conducting emeraldine salt phase **(18)**. The vibrating frequency at 1130 cm-1 was due to the C-H in plane bending vibration in quinoid ring and can be assigned to B-NH+=Q structure that formed during the protonation process **(32, 34)**. Palaniappan et al,**(19)** assigned this band as an electronic band as well as a high degree of electron delocalization. This band was expected due to the greater degree of oxidation and related to the doped structure. It increases with the degree of doping of polymer backbone and indicates the existence of positive charge on the chain inducing a dipole moment and the distribution of the dihedral angle between the quinone and benziod rings. The bands in the range 800–880 cm-1 was identified with the out-of-plane bending of C-H bond in the 1,4-disubstituted aromatic ring, which has been used as a key to identify the type of substituted benzene. The bands at 706, 617 and 590 cm-1 are associated with C-C bending vibrations in quinoid and benzenoid ring.

Macdiarmid et al,**(35)** assigned the two bands at 815, 706 cm-1 as a para-substituted aromatic ring and of ortho or meta substitution aromatic ring respectively. The presence of the bands at 706 cm-1 815 cm-1 in the infrared spectra indicated that; the polymerization has proceeded in a "head to tail" fashion. The locations of these characteristic peaks are in a good agreement with the literature **(18,36, 37)**.

INTERNATIONAL JOURNAL OF
ADVANCED SCIENTIFIC RESEARCH AND INNOVATION
ISSN: 2785-9541 VOLUME 2, ISSUE 1, 2021, 1 – 20. www.egyptfuture.org/ojs/

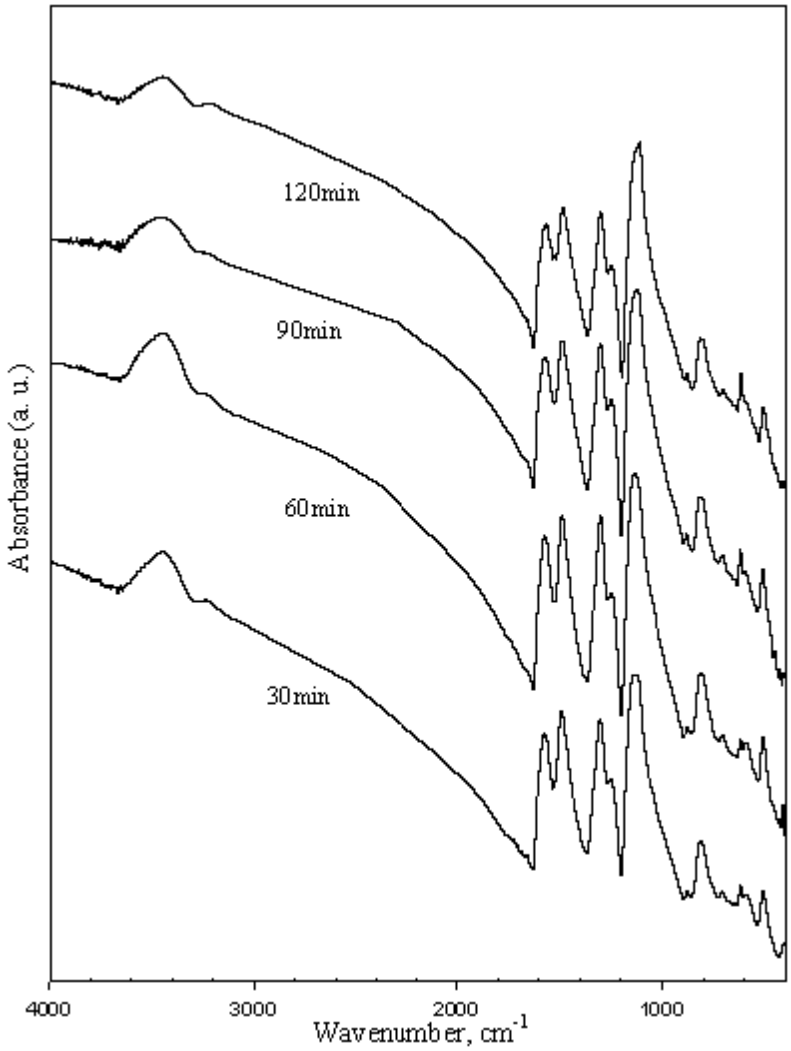

Figure (3): Infrared spectrum of doped polyaniline nanoparticles at different oxidation times from 30 min to 120 min.

3.1. Effect of oxidation time on the Infrared Spectra of PANI nanoparticles.

The effect of oxidation time on the infrared spectra of PANI nanoparticles was observed in Figure (3). As a general it was found that small shifts in the

ISSN: 2785-9541 VOLUME 2, ISSUE 1, 2021, 1 – 20. www.egyptfuture.org/ojs/

wavenumbers were happened for many bands and other peaks hardly shifted. Concretely, there is no shift in the band position of NH stretching vibration in the secondary amine at 3233 cm-1. By comparing the spectra of the samples prepared at oxidation times 60, 90 and 120 min (different particle size) with the spectrum of the sample prepared at 30 min it can be observed that the absorption band of N=Q=N at 1575 cm-1 for the quinonoid was shifted to 1573, 1570, 1564 cm-1 and the band of B-N-B at 1492 cm-1 for the benzenoid structures shifted to 1489, 1485, 1483 cm-1. These bathochromic shifts was happened due to the extended electronic conjugation length in PANI chain with increasing the particle size and the changes of environment at the molecular level. Sainz et al,**(38)** explained the red shift and it was related to indicative of a more semiquinoid form. The intensity ratio of the absorption band of quinonoid to benzenoid structure was calculated form Figure (3) using the following equation R (intensity ratio)=(***I*** N=Q=N cm−1/ ***I*** N-B-N cm-1); and it was shown in table (2). The change of intensity ratio with the oxidation state was shown in Figure (4). This ratio measure of the extent of oxidation state of the polymer and it was reflected to the content of the quinoid dimine and benzene ring structute **(18,39)**.The ratio is (0) for the fully reduced form, 0.5–1 for the protoemeraldine form, 1 for the partially oxidized form and >1 for the fully oxidized form**(36)**. From Table (2) and Figure (4) it is clear that the intensities of absorption ratio of I1575 to I1492 are increased with increasing oxidation times from 0.9306 5to 1.09228, which indicates that the benzeniod unit was changed to quinoid structure in PANI, also related to increase in

ISSN: 2785-9541 VOLUME 2, ISSUE 1, 2021, 1 – 20. www.egyptfuture.org/ojs/

oxidation state of polyaniline and nanoparticles was formed as the emeraldine salt form.

Table (2): Intensity Ratio of the IR bands of the qnionid structure to benzenoid structure for doped PANI prepared at different oxidation times.

PANI prepared at different oxidation time	Particle size (nm)	Ratio(I(N=Q=N)/I(N-B-N))
30 min	3.2	0.93065
60 min	5.5	0.95093
90 min	6.8	0.99548
120 min	10	1.09228

INTERNATIONAL JOURNAL OF
ADVANCED SCIENTIFIC RESEARCH AND INNOVATION
ISSN: 2785-9541 VOLUME 2, ISSUE 1, 2021, 1 – 20. www.egyptfuture.org/ojs/

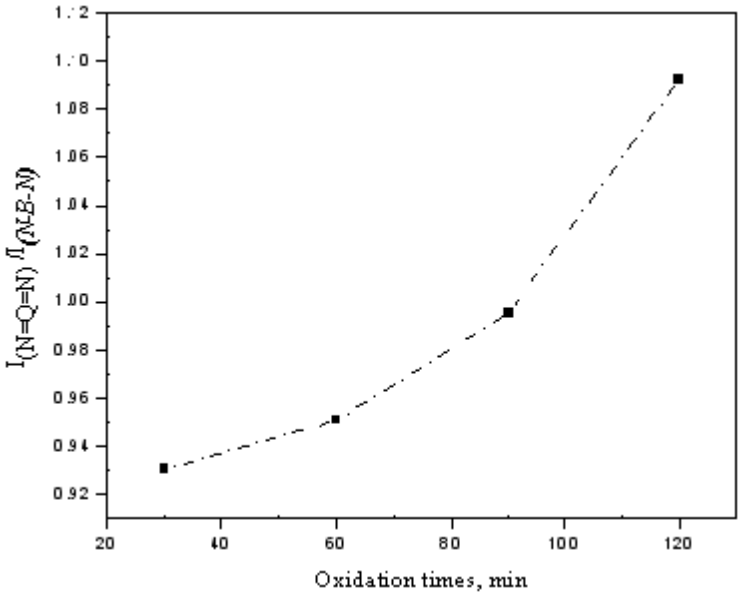

Figure (4): the intensity ratio of the quinonoid to benzenoid structure vs oxidation times.

4. UV-Visible spectra for different nanoparticles of PANI.

The ultraviolet visible (UV–VIS) spectra of the PANI nanoparticles prepared at different oxidation times under ultrasonic irradiation in DMF as a solvent were shown in Figure (5). It was found that, two characteristic absorption bands were appeared. These two bands were characterized doped PANI. The first characteristic band around 326 nm was related to π- π* transition of the benzene rings as well as this band assigned to the extent of conjugation between adjacent phenyl rings in the polymeric chains. The second band at 610 nm assigned to n-π* electronic transition of quinonoid ring. This band can be discussed as the charge transfer from the benzene rings to the quinoid

ISSN: 2785-9541 VOLUME 2, ISSUE 1, 2021, 1 – 20. www.egyptfuture.org/ojs/

with each side contributing on average ~ an electron to the quinoid ring. Our UV-VIS results agree with the literatures **(40-43).**

4.1. Effect of oxidation time on UV-VIS spectra of PANI

The strong dependence of UV-VIS spectra on nanoparticle size of PANI has been observed in Figure (5). Generally, intensity of the characteristic bands was increased with increasing the ultrasonic irradiation time. This may be due to the increase of the concentration of PANI in the reaction medium. By comparing the spectra of PANI prepared at oxidation times (30, 60, 90 and 120 min) Figure (5) it was observed that with increasing oxidation times, the two absorption bands at 326 nm and 610 nm were affected. There were slightly shifted towards higher wavelength (bathscromic shift) in the position. The band at 326 nm was shifted to 340 nm and the band at 610 shifted to 635 nm. This is may be due to the ring substitution and it was agreed with Lahiff et al, **(43)**. The data of TEM was indicated that, the PANI prepared at oxidation time of 120 min had the largest particle size (10 nm). The sample with this size was shifted to the maximum wavelength (red shift). This means that the red shift occurred with particle size increase PANI chain. In contrast, it can be seen that, the sample prepared at oxidation time of 30 min shows the maximum blue shift compared with the samples prepared at higher oxidation time. With increasing the particle size by increasing the oxidation times the absorbance shifted to higher wave length. This behavior could be attributed to the quantum confinement. All these may be due to the conjugation lengths of PANI was increased with increasing the oxidation time. The degree of oxidation can be estimated from the intensity ratio of the band at 610 nm (qnionid structure) to the band at 326 nm

ISSN: 2785-9541 VOLUME 2, ISSUE 1, 2021, 1 – 20. www.egyptfuture.org/ojs/

(benzenoid structure)**(43)** in Table (3). It is clear that the intensities of absorption ratio of I610 to I326 were increased with increasing oxidation times from 0.83065 to 0.94547. This means that the benzeniod unit changed into quinoid structure in PANI. Also, these results indicated the formation of PANI emeraldine salt (ES) form and it was agreed with the FTIR results.

Table (3): Ratio of the UV-VIS bands of the qnionid structure to benzenoid structure for doped PANI prepared at different oxidation time(43-45).

Time of oxidation	Particle size (nm)	Ratio (I610/I326)
30 min	3.2	0.83065
60 min	5.5	0.85093
90 min	6.8	0.91548
120 min	10	0.94547

INTERNATIONAL JOURNAL OF
ADVANCED SCIENTIFIC RESEARCH AND INNOVATION

ISSN: 2785-9541 VOLUME 2, ISSUE 1, 2021, 1 – 20. www.egyptfuture.org/ojs/

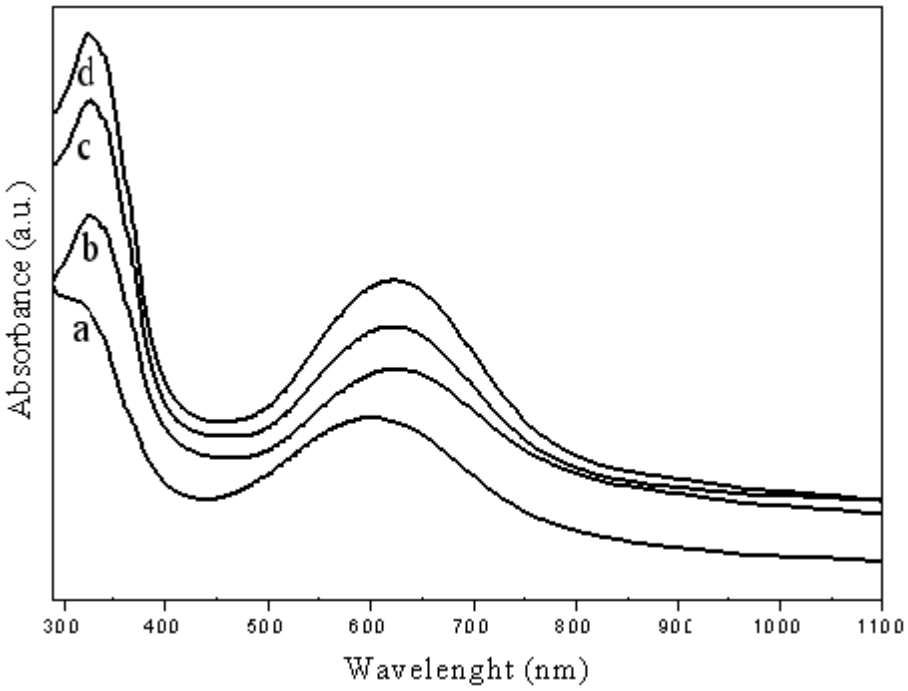

Figure (5): UV-Vis spectra of PANI nanoparticles at different oxidation times (a) 30 min, (b) 60 min, (c) 90 min and (d) 120 min in DMF solvent.

Conclusion

Different nanoparticle sizes and spherical shapes of PANI/Hcl nanoparticles were successfully formed using different time of ultrasonic irradiation. The particle sizes were increased from 3.2 to 10 nm and studied as a function of oxidation times. It was found that, the crystallinity of doped PANI nanoparticles was increased with increasing particle sizes. The FTIR and

ISSN: 2785-9541 VOLUME 2, ISSUE 1, 2021, 1 – 20. www.egyptfuture.org/ojs/

UV/VIS spectra data agreed with the TEM and XRD and all confirmed that PANI nanoparticle was prepared in emeraldine salt form.

References

1. Z. X. Wei, Z. M. Zhang, and M. X. Wan, Langmuir, 18(2002) 917.

2. B. J. Kim, S.G. Oh, M. G. Han, and S. S. Im, Synthetic Metals, 122 (2001) 297.

3. L. Meng, Y. Lu, X. Wang, J. Zhang, Y. Duan, and C. Li, Macromolecules, 40 (9) (2007) 2981.

4. A. R. Hopkinsa, D. D. Sawallb, R. M. Villahermosaa, and R. A. Lipelesa, Thin Solid Films, 469 (2004) 304.

5. T. M. Wu, Y. W. Lin, and C. S. Liao, Carbon., 43 (2005) 734.

6. S. Goel, A. Gupta, K. P. Singh, R. Mehrotra, and H. C. Kandpal, Materials Science and Engineering, A., 443 (2007) 71.

7. J. Huang, S. Virji, B. H. Weiller, and R. B. Kaner, J. Am. Chem. Soc., 125 (2003) 314.

8. J. Gao, J. M. Sansinena, and H. L. Wang, Chem. Mater., 15(2003**)** 2411.

9. J. Janata, and M. Josowicz, Nat. Mater., 2 **(**2003) 19.

10. C. G. Wu, and T. Bein, Science., 264(1994) 1757.

11. M. R. Anderson, B. R. Mattes, H. Reiss, and R. B. Kaner, Science., 252 (1991) 1412.

12. J. Yang, S. M. Burkinshaw, J. Zhou, A. P. Monkman, and P. J. Brown, Adv. Mater., 15 (2003)1081.

13. A. Baba, W.Knoll, Adv. Mater. 15(2003) 1015.

ISSN: 2785-9541 VOLUME 2, ISSUE 1, 2021, 1 – 20. www.egyptfuture.org/ojs/

14. C. R. Martin, in: T.A. Skotheim, R.L. Elsenbaumer, J.R. Reynolds (Eds.), Handbook of Conducting Polymers, 2nd ed., Marcel Dekker, New York, (1998) 409.

15. N.M. Farrage, A.H. Oraby, E.M.M. Abdelrazek and D. Atta, Biointerface Res. Appl. Chem, 9 (2019) 3934 - 3941

16. N.M. Farrage, A.H. Oraby, E.M.M. Abdelrazek and D. Atta, Egyptian Journal of Chemistry, 62 (2019) 99 – 109.

17. D. Atta, A. Okasha and M. Ibrahim, Der Pharma Chemica, 8 (2016) 76-82

18. T. Abdiryim, Z. X. Gang, and R. Jamal, Materials Chemistry and Physics, 90 (2005) 367.

19. S. Palaniappan and S. L. Devi, Polymer Degradation and Stability, 91 (2006) 2415.

20. S. Kumar, V. Singh ,S. Aggarwal, U. K. Mandal, and R. K. Kotnala, Composites Science and Technology, 70 (2010) 249.

21. O. Osman, A. Mahmoud, D. Atta, A. Okasha, and M. Ibrahim, Der Pharma Chemica, 7 (2015) 377-380.

23. O. O. Adetunji, The nature of electronic states in conducting polymer nano-networks, Graduate School of The Ohio State University, PhD thesis, (2008).

ISSN: 2785-9541 VOLUME 2, ISSUE 1, 2021, 1 – 20. www.egyptfuture.org/ojs/

24. S. Bhadra, and D. Khastgir, Polymer Degradation and Stability, 92 (2007) 1824.

25. S. Bhadra, N. K. Singha, and D. Khastgir, Polym, Int., 56 (2007) 919.

26. D. Kim, J. Choi, J. Y. Kim, Y. K. Han, and D. Sohn, Macromolecules, 35 (2002) 5314.

27. S. Bhadra, N. K. Singha, and D. Khastgir, European Polymer Journal, 44 (2008) 1763.

28. S. Zhou, T. Wu, and J. Kan, European Polymer Journal, 43 (2007) 395.

29. X. Bai, X. Li, N. Li, Y. Zuo, L. Wang, J. Li, and S. Qiu,Materials Science and Engineering, C., 27 (2007) 695.

30. S. A. Chen, and H. T. Lee, Macromolecules, 28 (1995) 2858.

31. Y. Furukawa, F. Ueda, Y. Hyodo, I. Harada, T. Nakajima, and T. Kawagoe, Macromolecules, 21 (1988) 1297.

32. H. Xia, J. Narayanan, D. Cheng, C. Xiao, X. Liu, and H. S. O. Chan, J. Phys. Chem. B., 109 (2005) 12677.

33. Y. Yu, S. Zhihuai, S. Chen, C. Bian, W. Chen, and G. Xue, Langmuir, 22 (2006) 3899.

34. X. Bai, X. Li, N. Li, Y. Zuo, L. Wang, J. Li, and S. Qiu,Materials Science and Engineering, C., 27 (2007) 695.

35. S. K. Manohar ,A. G. Macdiarmid, K. R. Cromack, J. M. Ginder, and A. J. Epstein, Synthetic Metals, 29 (1989) E349.

36. A. Parsa, and S. A. Ghani, Polymer, 49 (2008) 3702.

37. J. Kan, S. Zhang and G. Jing, Journal of Applied Polymer Science, 99 (2006) 1848.

ISSN: 2785-9541 VOLUME 2, ISSUE 1, 2021, 1 – 20. www.egyptfuture.org/ojs/

38. Y. H. Elshaer, D. Atta, M. A. M. El-Mansy, M. A. Hegazy, H. A. Ezzat and M. A. Ibrahim, Sensor Letters, 16(2018) 311-321.

39. D. Atta, A. Mahmoud, A. Fakhry, Biointerface Research in Applied Chemistry, 9 (2019) 3817 - 3824.

40. M.M. Ayad, N.A. Salahuddin, A.K. Abou-Seif, and M.O. Alghaysh, European Polymer Journal, 44 (2008) 426.

41. J. Kan, R. Lva and S. Zhang, Synthetic Metals, 145 (2004) 37.

42. R. Sainz, W. R. Small, N. A. Young, C. Valle´s, A. M. Benito, W. K. Maser, and M. I. H. Panhuis, Macromolecules, 39 (2006) 7324.

43. E. Lahiff , T. Woods, W. Blau, G. G. Wallace, and D. Diamond, Synthetic Metals, 159 (2009) 741.

44. A. A. Mahmoud, O. Osman, K. Eid, E. Al Ashkar, A. Okasha, D. Atta, M. Eid, Z. Abdel Aziz and A. Fakhry, Middle East Journal of Applied Sciences, 4 (2014) 816-824.

45. D. Atta, A. Fakhry and M. Ibrahim, Der Pharma Chemica, 7(2015) 357-361.